One-Dimensional Self-Assembled Molecular Chains on Cu(100): Interplay between Surface-Assisted Coordination Chemistry and Substrate Commensurability

Steven L. Tait,*,† Alexander Langner,† Nian Lin,† Sebastian Stepanow,† Chandrasekar Rajadurai,§ Mario Ruben,*,§ and Klaus Kern†,‡

Max Planck Institute for Solid State Research, Heisenbergstrasse 1, D-70569 Stuttgart, Germany, Forschungszentrum Karlsruhe, Institute for Nanotechnology, Postfach 3640, D-76021 Karlsruhe, Germany, and Institute de Physiques des Nanostructures, Ecole Polytechnique Fédérale de Lausanne, CH-1015 Lausanne, Switzerland

Received: February 8, 2007; In Final Form: May 16, 2007

The surface-assisted self-assembly of one-dimensional chains using linear, rigid bipyridyl molecules of different lengths on the Cu(100) surface is presented. The chains are assembled from a stable 2-fold coordination of the terminal pyridyl groups of the molecules with Cu adatoms which diffuse from the substrate step edges. This type of interaction is selective and reversible, allowing for effective self-assembly. We observe several partially dynamic aspects of chain growth which highlight critical considerations for growth of the present system as well as other molecular nanostructures on solid substrates. The steric and electronic templating of the metal substrate leads to strictly one-dimensional bonding geometries and unusually low (2-fold) coordination. The epitaxial relation of the molecular structure with the substrate lattice has profound effects on the growth kinetics and stability of the structures. Additionally, the substrate-mediated interactions influence the stability and structure over longer ranges than can be influenced by bonding interactions, manifested here as specific interchain distances at high molecule coverages.

I. Introduction

The design and construction of nanometer-scale structures at surfaces is currently a topic of intense research and high interest for the advancement of nanotechnology.[1] Construction of nanostructures at surfaces using organic molecules has the attractive advantages of being able to utilize tailor-made (synthesized) building blocks and to program the molecule interaction centers with specific orientations and strengths to provide a library of potential nanostructure geometries.[2] By using a bottom-up self-assembly approach, entire surfaces can be patterned with nearly uniform structures using specific organic or hybrid organic/metallic components and appropriate thermal conditions. Such a surface-assisted self-assembly approach has already yielded highly ordered supramolecular network structures using hydrogen bonding[3] or metal coordination of ligands such as carboxylates and pyridyls,[4−6] biphenols,[7] and *bis*-carbonitriles.[7] Furthermore, metal−terpyridine systems have recently been assembled at the solid/liquid interface.[8]

There have been several previous studies showing one-dimensional (1D) molecule chains on metal surfaces stabilized by hydrogen bonding or electrostatic interactions.[9,10] In those cases, the intermolecular interaction was typically established via rather weak hydrogen bonds involving aromatic C−H groups as donors. Stronger metal−organic ligand coordination bonds have been used to stabilize molecular chains, but there the 1D molecule growth was guided by the Cu(110) surface anisotropy.[11]

Here we present results of 1D molecular nanostructures stabilized by 2-fold linear metal−ligand coordination. Two different linear organic ligands terminated by pyridyl groups, 1,4-bis(4-pyridyl)benzene (**1**) and 4,4′-bis(4-pyridyl)biphenyl (**2**) (see Figure 1), were used in the self-assembly processes. Such bifunctional ligands belong to the large family of aromatic nitrogen heterocycles, which have been demonstrated to be effective ligands for transition metal coordination in bulk supramolecular chemistry.[12−15] There, it was shown that both ligands form an open square-grid two-dimensional (2D) coordination polymer with $Ni(NO_3)_2$[14] and that **2** yields three types of different polymers (2D square-grid, double linear chain, and linear chain) with $Cd(NO_3)_2$ in a single crystal.[12] We find that **1** and **2** each form 1D chain structures stabilized by 2-fold linear coordination bonding with the inherent Cu adatom population on the Cu(100) surface at room temperature. The relative stabilities of these structures illustrate the interplay between the chain bonding motif and substrate commensurability, illustrating critical issues for the design of supramolecular structures at surfaces.

II. Experimental Section

All experiments were performed in ultrahigh vacuum systems with base pressures of $<2 \times 10^{-10}$ mbar. The Cu(100) surface was cleaned by repeated cycles of sputtering with 500 eV Ar ions and annealing to 800 K. Scanning tunneling microscopy (STM) was performed using two different microscopes in two separate, but similar, vacuum systems. In each experiment the sample was prepared in the corresponding vacuum system and not exposed to atmosphere. One STM operates at room temperature and the other system is cooled by a liquid helium cryostat so that the sample and STM temperature during measurement are approximately 5 K. The effect of STM scanning on the molecules and coordination structures is negligible at the modest tip biases (<1 V) and low tunneling

* E-mail: S.Tait@fkf.mpg.de; Mario.Ruben@int.fzk.de.
† Max Planck Institute for Solid State Research.
‡ Ecole Polytechnique Fédérale de Lausanne.
§ Forschungszentrum Karlsruhe.

10.1021/jp071100v CCC: $37.00
Published on Web 07/04/2007

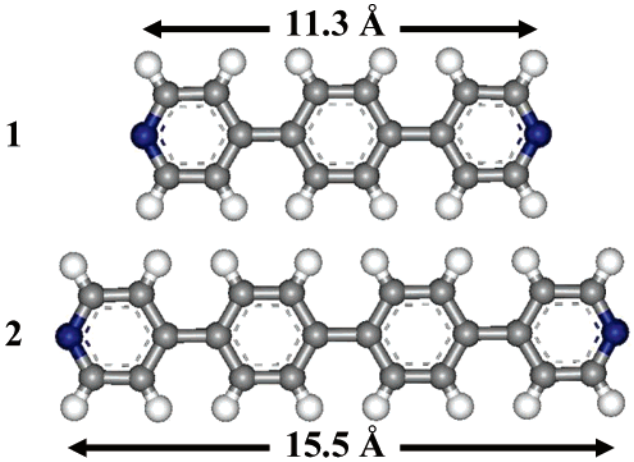

Figure 1. Molecular structure of the ligands 1,4-bis(4-pyridyl)benzene, **1**, and 4,4′-bis(4-pyridyl)biphenyl, **2**, exhibiting different distances between the nitrogen atoms. Color scheme: N = blue, C = gray, H = white.

currents (~0.1 nA) used in this study. Distance measurements from each STM have been calibrated to known structures.

The ligands 1,4-bipyridyl-benzene (**1**) and 4,4′-bipyridyl-biphenyl (**2**) are illustrated in Figure 1 and were prepared following reported procedures.[14,15] The molecules are sublimed from a Knudsen-cell type evaporator at temperatures of 400 and 450 K, respectively, in each case giving a molecule flux of approximately 0.1−0.2 monolayers/min at the sample. The Cu(100) substrate is at room temperature during molecule deposition. The interaction of aromatic molecule adsorbates with metal substrates is primarily expected to be between the molecule π-system and the substrate d-electrons, causing the molecule backbone rings to be approximately parallel to the surface plane and the molecule center to be close to the substrate to maximize dispersion forces.[16]

III. Self-Assembly of 1

Upon deposition at room temperature, it is observed that the molecules of **1** self-assemble into one-dimensional chains, as shown in Figure 2. These chains are determined to be stabilized by metal−organic coordination interactions based on several observations. Due to the presence of electron lone pairs at the terminal nitrogen groups of **1**, an end-to-end molecule interaction would be repulsive. Cu adatoms, available by evaporation from the step edges at room temperature on Cu(100),[17] can coordinate the pyridyl endgroups of the adjacent molecules to stabilize the chain structure. The chains exhibit a segment length that is considerably longer than the size of the molecule, as illustrated by the molecular model (drawn to the scale of the STM data) in Figure 2a. The chain segment length is measured in the STM to be 15.1 ± 0.1 Å and the molecule length is only 11.3 Å, allowing a pyridyl−Cu−pyridyl coordination. (STM measurements of chain segment lengths are given as an average ± 1 standard deviation of many chain measurements from different STM micrographs.) This scenario is also supported by the observation that in the absence of Cu adatoms [e.g., on a Ag(111) substrate] such chains do not exist.[18] The estimated Cu−N bond length is 1.9 Å, which is in good agreement with similar bond lengths in three-dimensional (3D) coordination compounds, as discussed below. The Cu centers are not resolved in this STM measurement presumably due to the electronic effect which was reported before.[11]

A 2-fold coordination between pyridyl groups and Cu centers has not been observed in bulk coordination chemistry. There

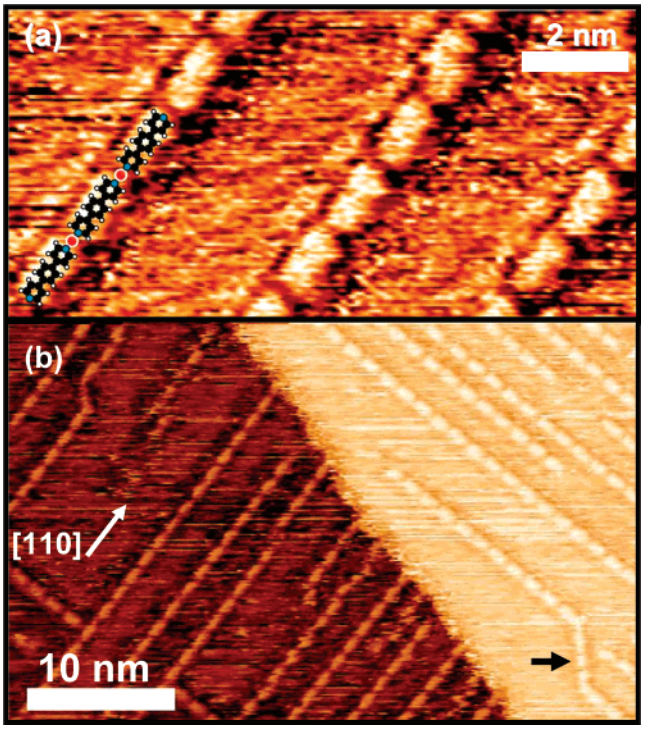

Figure 2. STM images of **1** adsorbed on Cu(100) and imaged by STM at 300 K: (a) detail of **1**−Cu chains with a structural model illustrating N−Cu−N coordination bonding (Cu centers red with white highlight) and (b) overview of **1**−Cu chains attached to the lower side of the terrace step or running parallel on the upper side of the step. The black arrow in b indicates a short chain segment running in the [100] direction, as discussed in text.

Cu(I) ions coordinated exclusively to pyridine ligand groups prefer a quasi-tetrahedral configuration while Cu(II) leads mainly to Jahn−Teller distorted square-pyramidal, or sometimes pseudo-octahedral, coordination motifs.[19] Linear coordination of pyridine ligands around a Cu dimer has been observed in solution, but with the Cu ions bearing additional ligands equatorially.[20] However on a surface a 2-fold linear coordination is not unexpected, since it was shown previously in the case of the coordination of iron and copper centers with carboxylates that the presence of the substrate plays in favor of lowered coordination numbers.[4,21] Those experimental studies are also supported by ab initio DFT calculations.[6]

The coordination differences in the present case from the 3D coordination chemistry expectations can primarily be attributed to the steric influence of the substrate. As with most aromatic compounds adsorbed on metal surfaces,[9,22] the molecule **1** is expected to adsorb on the Cu(100) surface with its backbone approximately parallel to the substrate. With the molecule confined to a 2D planar geometry, the coordination options are limited. At higher coordination numbers, the ligand−metal bond length would be too large (>3 Å) due to repulsive interactions between the molecule backbones, especially the α-protons, of the involved ligands. Only a 2-fold coordination is feasible due to this steric crowding of the ligands being fixed in a plane. However, the availability of the underlying substrate atoms to interact electronically with the coordinated Cu center can also serve to satisfy the coordination of the metal center.[6] This can contribute to charge balancing by screening effects and lead to image charges in the substrate. In our study, we do not have a direct measure of the ionization state of the Cu center, but whatever charge state is necessary can be balanced by the infinite charge reservoir of the substrate.

As shown in Figure 2b, most of the **1**−Cu chains nucleate at the lower side of the atomic step edges on the surface and extend almost completely across the terraces. On the upper side of the terrace step edges, the chains prefer a parallel orientation with respect to the step edge. Two-thirds of the molecules reside in chains that are attached to the step edges, and so approximately the same fraction of the terrace area is taken up by those chains. The interface between these regions contains some 'T'-intersections between the two chain directions. The chains are oriented in the [110] or [1$\bar{1}$0] direction of the Cu substrate. This orientation apparently allows for a preferred adsorption geometry for the molecule−Cu adatom chain complex. The molecule axis is oriented parallel to the chain direction. There are also a small number of molecules in short chains (typically only 2−3 molecules long) which are oriented in the [100] direction (e.g., the short segment marked by the black arrow in Figure 2b). These are exclusively observed when both ends terminate at junctions with chains in the [110] direction.

The 1D coordination chains in the [110] direction very clearly exhibit the reversibility of the N−Cu−N complexation. This reversibility is a critical ingredient for successful self-assembly[23] as it allows for growth of uniform structural domains as well as error correction within the assembly. The reversibility of the binding of these chains at room temperature is manifest in our experiments as constant morphological evolution of the chains with time. The apparent 'noise' in the room temperature STM data is primarily attributed to mobile admolecules interacting briefly and randomly with the scanning tip. This gives rise to bright streaks along the fast scan direction of the images as well as brief spikes in the tunneling current, imaged as small spots in the STM data. In time sequences of STM images, separated by several minutes, we observe the dissolution of some chains and growth of others as well as nucleation of completely new chains. There appears to be a 2D quasi-equilibrium on the surface between the 1D condensed phase of the molecules and a 2D mobile molecule phase. This allows poorly formed chains ([100] direction, missing Cu centers, etc.) or poorly positioned chains (too close to neighbor chains, intersection with perpendicular chains, etc.) to dissolve and their constituents to participate in the growth of a more energetically favorable chain. This also allows for regions of parallel chains to evolve on the surface, vide infra, rather than a random distribution of chain orientations. The many chains growing parallel to one another, even away from the step edges, is a strong indication of the reversibility of the Cu−pyridyl coordination complexes which allows the chains to grow and orient themselves in the most energetically favorable configuration.

IV. Self-Assembly of 2

We have also investigated the structure of molecule **2** on the Cu(100) surface at room temperature (Figure 3a). This molecule is identical to molecule **1** except that the backbone of the molecule is lengthened by one phenyl ring (see Figure 1). We note that the coordination sites of these two molecules are identical. If one would consider the coordination bonding of these molecules to Cu centers in the absence of the atomic lattice (i.e., no adsorbate−substrate potential corrugation parallel to surface), the bonding geometry and coordination of each of the molecules to Cu centers must be identical. It is therefore interesting to note that while molecule **2** also condenses on the Cu(100) substrate in 1D structures, the growth mode, especially the stability of the structure, is significantly different from the shorter molecule **1**. The STM image in Figure 3a is very noisy due to mobile molecules moving under the scanning tip,

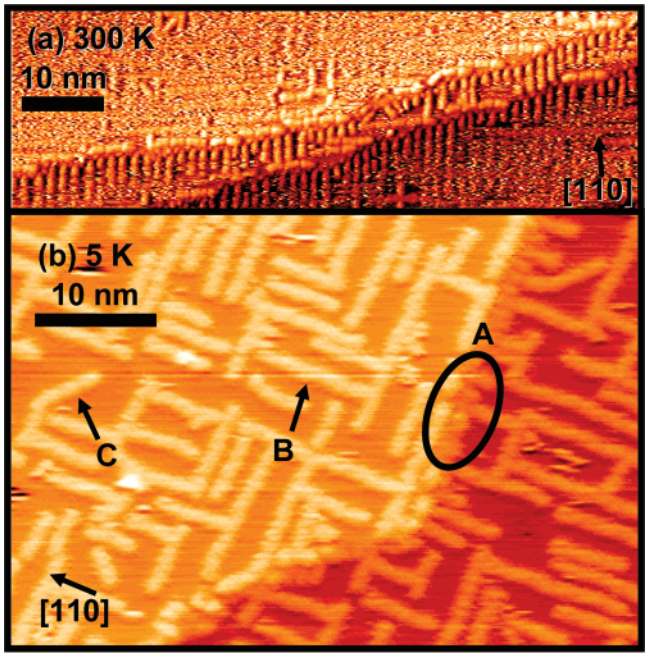

Figure 3. STM images of **2** assembled at the Cu(100) surface at 300 K and measured by STM at (a) 300 K and (b) 5 K. (a) Lower step edges saturated with short chain structures. Image noise due to mobile molecules moving under the STM tip. (b) Lower side of steps saturated with molecules (A). Two 1D chain structures: (B) majority structure stabilized by Cu−N coordination bonding and (C) stabilized by C−H···N hydrogen bonding. C is oriented at 45° to B and has a shorter segment length.

indicating that many molecules are mobile on the terraces rather than condensing into the **2**−Cu chains at this temperature.

Compared with **1**, the coordination chains of the longer molecule **2** show a preference for much shorter chain growth, but they still prefer nucleation at the lower side of the Cu step edges. Generally, they populate the step edges at a much higher density than molecule **1**. We see in Figure 3a that the lower sides of the Cu atomic step edges are almost completely saturated with molecules of **2**, but the chains originating from the step edges do not show significant growth. This is a sharp contrast to the growth of the long, parallel chains of **1**−Cu. Apparently the stability of **2** in the 1D chains is lower than that of **1**, producing a larger population of **2** attached to the step edges or mobile in a 2D gas phase. Along the upper side of the step edge there are molecule chains running parallel to the step edge. These chains are typically short, on the order of 3−5 molecules long. There is not a continuous chain along the upper side of the step edge but rather a series of chain fragments with small offsets from one another. This appears to be due to the molecules adsorbing along the [110] direction of the Cu substrate, even though the mean direction of this step edge deviates slightly from the low-energy [110] direction. It is also noteworthy that the density of the chains is significantly higher at the lower side of the terrace step edge compared to the upper side. This again indicates that the step edge atoms are good coordination sites for the nucleation and growth of the chains.

In order to reveal the stable assembly of molecule **2**, low-temperature measurements were performed. The molecule was evaporated onto the Cu(100) surface at room temperature and then cooled to 5 K for STM imaging (Figure 3b). As the temperature of the sample is cooled from room temperature, adsorbate mobility becomes essentially zero allowing us to visualize the condensed states of the molecules clearly. Three general structures into which the molecules of **2** have condensed

are observed on the Cu(100) surface and labeled in Figure 3b. The terrace steps are decorated with a very high density of molecules or short molecular chains (typically only 1−5 molecules) leading to a complete saturation of the lower side of the step edges, nearly identical to the step-edge decoration at room temperature (ellipse 'A' in Figure 3b).

On the terraces of the substrate two types of molecular chains can be observed, which can be distinguished by their orientation relative to the substrate as well as by the chain segment length, measured by STM.

The predominant chains exhibit a segment length of 19.5 ± 0.2 Å and are oriented along the [110] direction (labeled 'B' in Figure 3b). These seem to be a longer version of the **2**−Cu chains observed at room temperature. These chains are also similar in substrate orientation and in their growth into the terraces to the chains formed by the molecule **1** at room temperature, except that many of these chains are not attached to the step edges but have nucleated in the centers of the terraces. Also, the chains of the molecule **2** have a shorter average length and a broader distribution of chain lengths.

The other type of chain, occurring much less frequently (accounting for <2 % of the molecules), has a significantly shorter chain segment distance of 15.9 ± 0.1 Å (labeled 'C' in Figure 3b). These are oriented in the [100] direction (i.e., at 45° to the [110] terrace step edges). The chain segment length compared to the molecule length of 15.5 Å indicates that there is not sufficient space within these chains for the molecules to be stabilized by Cu-coordinated bonding. Therefore it is proposed that these chains are stabilized by intermolecular hydrogen bonding interactions of the α-C−H proton of the pyridyl ring to the lone pair of a nitrogen of a neighboring molecule with the molecule axis rotated slightly from the chain direction. The shorter chains of **1** that orient in the [100] direction are stabilized by the same type of hydrogen bonds. A hydrogen bonding motif such as this is generally considered quite weak in bulk structures,[24] but in the present near-surface conditions templating of the substrate might stabilize such less-favored bonds. This atypical bonding merits further discussion and will be the subject of a forthcoming article.[18] The 45° chains account for only a small fraction of the molecules of **2** in chains at low temperature and most likely represent those molecules left without a metal coordination center as the Cu adatom population on the surface decreases with decreasing temperature.

V. Discussion

The difference in the stability of the related Cu−pyridyl coordination chain species for the molecules **1** and **2** warrants further discussion of the commensurability of these structures with the Cu(100) surface.

For the coordination chains of molecule **1**, the STM results show that the molecules are perpendicular to the step edges. Each chain segment in the **1**−Cu chains is measured to be 15.1 ± 0.1 Å long, corresponding to 6 times the Cu nearest neighbor distance (2.55 Å = $a/\sqrt{2}$, Cu lattice constant a = 3.61 Å). This epitaxial agreement allows each Cu center in the chain to reside in the same adsorption geometry, most likely in the 4-fold hollow sites (energetically favored for Cu adatoms). The chain can nucleate at a Cu center in a step edge, and then growth proceeds with each molecule coordinated to a Cu center at each of its ends and the Cu centers each resting in hollow sites on the surface, as illustrated in Figure 4a. The Cu centers are separated along the [110] direction by six nearest neighbor distances, or 15.3 Å. That is, every sixth hollow site along the [110] direction is occupied by a Cu center, and the intervening spaces are filled by the molecules of **1**.

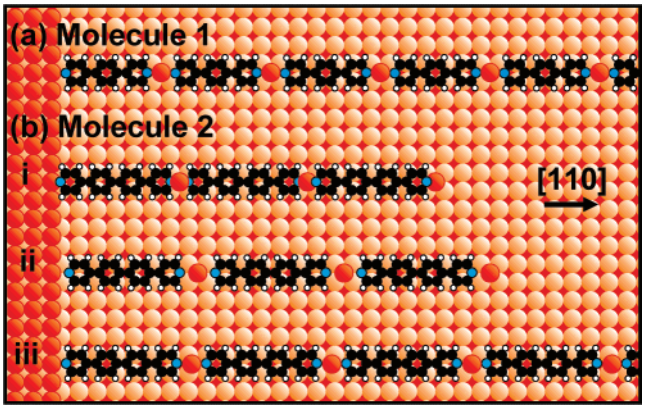

Figure 4. Models of 1D chain growth of (a) **1** and (b) **2** on Cu(100). Cu atoms in the upper layer (step edge or adatoms) are darker in color compared to those in the lower substrate layer. (a) Model for **1**−Cu coordination chains of periodicity 6 Cu nearest neighbor distances, d ($6d$ = 15.3 Å). (b) Models for **2**−Cu coordination chains. Chains i and ii have periodicities of $7d$ and $8d$, neither of which provide a suitable model. Chain iii agrees best with the STM results. Every third Cu atom along the chain is in a 4-fold hollow site, and the chain periodicity is $7\,{}^{2}/_{3}d$ (19.6 Å).

This model allows a Cu−N coordination bonding distance of 2.0 Å, consistent with expected values. In 3D (solution-based) coordination chemistry, Cu(I) ions tetrahedrally coordinated to pyridyl groups show average Cu−N bond distances in the range 1.9−2.2 Å.[19,25] Dicopper(II) ions axially coordinated to pyridyl groups and equatorially coordinated to carboxylate groups (octahedral geometry) exhibit Cu−N bond distances of ∼2.2 Å.[26]

A similar model for the 1D chain structure of the molecule **2** is also considered. As noted above, the bonding geometry and interaction potential for this molecule with Cu coordination centers should be identical to that of the shorter molecule. The difference in the growth of these molecules must therefore be due to the change in the commensurability of the coordination bonded chain structure with the substrate. While the **1**−Cu chain structure allows that the Cu centers sit in every sixth hollow site which allows for a stable Cu−N bond length of 2.0 Å, the chains involving molecule **2** do not permit all of the Cu centers to reside in identical favored adsorption sites, due to the mismatch of the molecule length and the substrate lattice. For example, we consider a structure similar to the **1**−Cu chains for the **2**−Cu chains with the Cu centers in every seventh or every eighth hollow site along the [110] direction (see Figure 4b, chains i and ii, respectively). These give chain segment lengths of 17.9 and 20.4 Å and Cu−N bond distances of 1.2 and 2.5 Å. The shorter configuration would not allow for a stable coordination bonding as the interaction would be strongly repulsive. The longer configuration is more reasonable, but the Cu−pyridyl interaction would be weak at such a long bond distance.

From our STM data, we measure a chain segment length of 19.5 ± 0.2 Å in the copper coordination chains of **2**. This distance agrees best with a high-order commensurate structure,[27] illustrated in chain iii of Figure 4b. We consider every third Cu center along the chain to be residing in a 4-fold hollow site, and the other Cu centers to be sitting slightly away from 2-fold bridge sites. That is, the Cu centers occupy every 23rd hollow site along the [110] direction and in between are two Cu centers, each sitting at a position between a bridge site and a hollow site, to form this high-order commensurate structure. The Cu−Cu distance along the chain is then 19.6 Å, and the Cu−N bond distance is 2.2 Å. This chain segment length corresponds almost exactly with the measured distance in the STM, indicating that

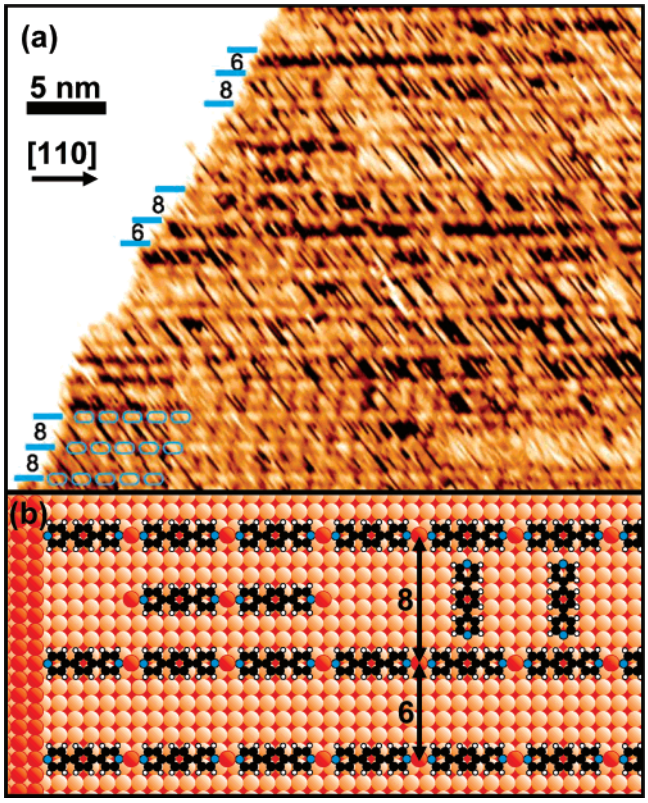

Figure 5. (a) Room temperature STM image of **1** on Cu(100) at high molecule coverage. A dense concentration of parallel 1D chains is attached to the step edge. The image has been rotated so that these chains are horizontal. Some chains are indicated by blue hash marks or blue ovals. (b) Model of chain structures. Labels '8' and '6' indicate chain separations of 8*d* or 6*d*. Many of the former have a less stable intermediate row. Chain separations labeled '6' do not have an intermediate row and represent the smallest stable chain spacing.

the energy cost of perturbing the Cu centers from their most favorable adsorption sites is compensated by a more favorable coordination bond geometry. However, the overall stability of this chain structure is reduced compared to the regular commensurate **1**−Cu chain structure. We conclude from this that the commensurability of the chain structure with the substrate has a very significant influence on the stability of the structure. This highlights the importance of considering the substrate interaction for the design and construction of nanometer-scale molecular systems.

VI. Interchain Interactions

The role of interchain interactions can be addressed by observing the growth behavior of the chains at different molecule coverages. The chain separation distances can be quantified as integer multiples of the Cu nearest neighbor distance, *d*, which is 2.55 Å. At low molecule coverages, the chains are separated by large distances ($\geq 8d$), indicating no appreciable interchain attraction. The frequency of chain separation distances decreases with increasing separation distance, but there are almost no chains with a closer separation distance than 8*d* until we increase the molecule coverage.

At high molecule coverage a regular finite spacing between the chains is observed. Figure 5a shows an STM micrograph of a high coverage of molecule **1** on Cu(100) at room temperature. The region shown is the lower side of a terrace step, and the white region at the left indicates the location of the upper step edge. At the lower side of the step edge, the stable chains seem to prefer an interchain distance of 8*d* or 6*d*. In most of the cases where two stable chains are separated by 8*d*, there is an intermediate chain between these that appears to be less stable (i.e., more mobile and discontinuous). Due to their rapid motion along these "nanochannels," the molecules in the intermediate chains appear as noisy blurs and are not well resolved by the STM (compared to the molecular resolution in the more stable chains), thereby causing the overall quality of Figure 5a to appear noisy. This 8*d* separation is labeled for four such instances in Figure 5a and also as a model in Figure 5b. It seems that the more rigid chains form a sort of nanochannel where the molecules can fill in, forming the intermediate chain, but only in a weakly stable configuration. It is not clear from the STM data what the exact structure of these less-stable intermediate chains is. However, we do see in the STM images that these chains have breaks in them at the same intervals as the neighboring coordination chains. We also observe that the less-stable chains do not generally have an attachment to the step edges. These chains appear broad in the STM, i.e., wider than the stable chains in the direction perpendicular to the channel direction. We consider two models for this structure, both illustrated in Figure 5b. Most likely the intermediate chains are simply molecules filling the channel and attaching to the rigid chains via hydrogen bond or electrostatic interactions. We cannot exclude the possibility that these intermediate chains are also coordination structures but made less stable by the close interchain distance. Both models support the observation of regular gaps in the chains which are commensurate with neighboring chains, and the first model clearly agrees with the observation of less step edge attachment and a lower stability compared to the neighboring chains. The filling of these channels gives what we consider to be the maximum monolayer density for these chains (2 molecules per $6d \times 8d$ unit cell = 1 molecule/156 Å^2). This spacing is illustrated in the top three rows of Figure 5b.

There are also stable chains with a separation of 6 Cu nearest neighbor distances, two of which are indicated along the left side of Figure 5a. This interchain spacing is illustrated between the last two chains of Figure 5b. In these cases, we do not observe an intermediate row of molecules in the STM data, and the STM image is smooth in these empty channels. In short, the chains seem to prefer a separation distance of 8*d* but still show stability at a separation of 6*d* and exhibit instabilities when the separation is further reduced.

For molecule **2** (cf. Figure 3), the average chain spacing of the densely packed chains at the lower side of the step edge is about 5*d* (12.8 Å). At 5 K (Figure 3b), the chain separation distance on the terraces is asymmetrically peaked around 6−7*d*, with very few chains having a closer separation (minimum separation of 4*d*) and the distribution of chains gradually decreasing with longer chain separation distances.

Repulsion between the molecule backbones can be excluded as the cause of the finite chain spacing because of the large distance between the chains (cf. Figure 5b). We propose that an electronic modification in the Cu surface due to the adsorption of the stable chains regulates the interchain separation, as has been observed for other cases of aromatic molecule adsorption on metals.[22] Another explanation could be a local structural reconstruction of the substrate induced by the strain of the molecule chain formation which affects the ability of additional chains to nucleate nearby. Similar surface-mediated elasticity effects have been observed in other long-range spatially ordered systems on metal substrate.[28] Both of these effects are known to account for regular spacing of 1D structures at metal surfaces.[29]

VII. Conclusions

We have shown self-assembly of 1D metal−organic chains stabilized by 2-fold linear coordination bonding with copper metal centers on an isotropic substrate. We have shown that by adjusting the chain structure commensurability with the substrate (accomplished here by using two similar molecules of different length) the stability and structure of the chains is strongly affected. We have also shown that at high coverages the coordination chains exhibit specific minimum chain separation distances. Several critical aspects of the substrate influence on supramolecular coordination structures—including commensurability effects on growth and stability, substrate-mediated repulsion between molecule chains, and low coordination numbers for metal−organic coordination bonding—have been highlighted. These systems show excellent properties for self-assembly including selectivity, recognition, and reversible binding. The structures expand the known library of coordination binding for the construction of nanometer-scale 1D structures at surfaces.

Acknowledgment. This work was partially supported by the EC-FP VI STREP "BIOMACH" (NMP4-CT-2003-505-487) and by the ESF-EUROCORES-SONS project "FunSMARTs". S.L.T. gratefully acknowledges support from the Alexander von Humboldt Foundation.

References and Notes

(1) Barth, J. V.; Costantini, G.; Kern, K. *Nature* **2005**, *437*, 671. Rosei, F. *J. Phys.: Condens. Matter* **2004**, *16*, S1373. Shchukin, V. A.; Bimberg, D. *Rev. Mod. Phys.* **1999**, *71*, 1125. Ruben, M. *Angew. Chem., Int. Ed.* **2005**, *44*, 1594.

(2) Barlow, S. M.; Raval, R. *Surf. Sci. Rep.* **2003**, *50*, 201. Rosei, F.; Schunack, M.; Naitoh, Y.; Jiang, P.; Gourdon, A.; Laegsgaard, E.; Stensgaard, I.; Joachim, C.; Besenbacher, F. *Prog. Surf. Sci.* **2003**, *71*, 95.

(3) Ruben, M.; Payer, D.; Landa, A.; Comisso, A.; Gattinoni, C.; Lin, N.; Collin, J. P.; Sauvage, J. P.; De Vita, A.; Kern, K. *J. Am. Chem. Soc.* **2006**, *128*, 15644. Pawin, G.; Wong, K. L.; Kwon, K. Y.; Bartels, L. *Science* **2006**, *313*, 961. Stohr, M.; Wahl, M.; Galka, C. H.; Riehm, T.; Jung, T. A.; Gade, L. H. *Angew. Chem., Int. Ed.* **2005**, *44*, 7394. Yan, H. J.; Lu, J.; Wan, L. J.; Bai, C. L. *J. Phys. Chem. B* **2004**, *108*, 11251. Griessl, S. J. H.; Lackinger, M.; Jamitzky, F.; Markert, T.; Hietschold, M.; Heckl, W. M. *J. Phys. Chem. B* **2004**, *108*, 11556. De Feyter, S.; Gesquiere, A.; Klapper, M.; Mullen, K.; De Schryver, F. C. *Nano Lett.* **2003**, *3*, 1485. Theobald, J. A.; Oxtoby, N. S.; Phillips, M. A.; Champness, N. R.; Beton, P. H. *Nature* **2003**, *424*, 1029. Stepanow, S.; Lin, N.; Vidal, F.; Landa, A.; Ruben, M.; Barth, J. V.; Kern, K. *Nano Lett.* **2005**, *5*, 901. Payer, D.; Comisso, A.; Dmitriev, A.; Strunskus, T.; Lin, N.; Woll, C.; DeVita, A.; Barth, J. V.; Kern, K. *Chem. Eur. J.* **2007**, *13*, 3900.

(4) Lingenfelder, M. A.; Spillmann, H.; Dmitriev, A.; Stepanow, S.; Lin, N.; Barth, J. V.; Kern, K. *Chem. Eur. J.* **2004**, *10*, 1913.

(5) Stepanow, S.; Lingenfelder, M.; Dmitriev, A.; Spillmann, H.; Delvigne, E.; Lin, N.; Deng, X. B.; Cai, C. Z.; Barth, J. V.; Kern, K. *Nat. Mater.* **2004**, *3*, 229. Stepanow, S.; Lin, N.; Barth, J. V.; Kern, K. *J. Phys. Chem. B* **2006**, *110*, 23472. Clair, S.; Pons, S.; Fabris, S.; Baroni, S.; Brune, H.; Kern, K.; Barth, J. V. *J. Phys. Chem. B* **2006**, *110*, 5627. Lin, N.; Stepanow, S.; Vidal, F.; Barth, J. V.; Kern, K. *Chem. Comm.* **2005**, 1681. Dmitriev, A.; Spillmann, H.; Lin, N.; Barth, J. V.; Kern, K. *Angew. Chem., Int. Ed.* **2003**, *42*, 2670. Lin, N.; Stepanow, S.; Vidal, F.; Kern, K.; Alam, M. S.; Stromsdorfer, S.; Dremov, V.; Muller, P.; Landa, A.; Ruben, M. *Dalton Trans.* **2006**, 2794.

(6) Seitsonen, A. P.; Lingenfelder, M.; Spillmann, H.; Dmitriev, A.; Stepanow, S.; Lin, N.; Kern, K.; Barth, J. V. *J. Am. Chem. Soc.* **2006**, *128*, 5634.

(7) Stepanow, S.; Lin, N.; Payer, D.; Schlickum, A.; Klappenberger, G.; Zoppellaro, G.; Ruben, M.; Brune, H.; Barth, J. V.; Kern, K. *Angew. Chem., Int. Ed.* **2007**, *46*, 710.

(8) Surin, M.; Samori, P.; Jouaiti, A.; Kyritsakas, N.; Hosseini, M. W. *Angew. Chem., Int. Ed.* **2006**, *46*, 245.

(9) Bohringer, M.; Morgenstern, K.; Schneider, W. D.; Wuhn, M.; Woll, C.; Berndt, R. *Surf. Sci.* **2000**, *444*, 199.

(10) Chen, Q.; Frankel, D. J.; Richardson, N. V. *Langmuir* **2002**, *18*, 3219. Furukawa, M.; Tanaka, H.; Kawai, T. *Surf. Sci.* **2000**, *445*, 1. Weckesser, J.; De Vita, A.; Barth, J. V.; Cai, C.; Kern, K. *Phys. Rev. Lett.* **2001**, *8709*, 096101. Humblot, V.; Barlow, S. M.; Raval, R. *Prog. Surf. Sci.* **2004**, *76*, 1. Barth, J. V.; Weckesser, J.; Cai, C. Z.; Gunter, P.; Burgi, L.; Jeandupeux, O.; Kern, K. *Angew. Chem., Int. Ed.* **2000**, *39*, 1230.

(11) Classen, T.; Fratesi, G.; Costantini, G.; Fabris, S.; Stadler, F. L.; Kim, C.; de Gironcoli, S.; Baroni, S.; Kern, K. *Angew. Chem., Int. Ed.* **2005**, *44*, 6142.

(12) Biradha, K.; Fujita, M. *Chem. Commun.* **2002**, 1866.

(13) Biradha, K.; Fujita, M. *Chem. Commun.* **2001**, 15; Steel, P. J. *Coord. Chem. Rev.* **1990**, *106*, 227.

(14) Biradha, K.; Hongo, Y.; Fujita, M. *Angew. Chem., Int. Ed.* **2000**, *39*, 3843.

(15) Fujita, M.; Oka, H.; Ogura, K. *Tetrahedron Lett.* **1995**, *36*, 5247.

(16) Witte, G.; Woll, C. *J. Mater. Res.* **2004**, *19*, 1889.

(17) Lin, N.; Payer, D.; Dmitriev, A.; Strunskus, T.; Woll, C.; Barth, J. V.; Kern, K. *Angew. Chem., Int. Ed.* **2005**, *2005*, 1488. Lin, N.; Dmitriev, A.; Weckesser, J.; Barth, J. V.; Kern, K. *Angew. Chem., Int. Ed.* **2002**, *41*, 4779.

(18) Tait, S. L.; Langner, A.; Lin, N.; Rajadurai, C.; Ruben, M.; Kern, K. In preparation.

(19) Osako, T.; Tachi, Y.; Taki, M.; Fukuzumi, S.; Itoh, S. *Inorg. Chem.* **2001**, *40*, 6604. Burke, P. J.; McMillin, D. R.; Robinson, W. R. *Inorg. Chem.* **1980**, *19*, 1211. Greenwood, N. N.; Earnshaw, A. *Chemie der Elemente*, 1st ed.; VCH: Weinheim, 1988. Dietrich-Buchecker, C. O.; Guilhem, J.; Pascard, C.; Sauvage, J. P. *Angew. Chem., Int. Ed.* **1990**, *29*, 1154.

(20) Biradha, K.; Sarkar, M.; Rajput, L. *Chem. Commun.* **2006**, 4169.

(21) Messina, P.; Dmitriev, A.; Lin, N.; Spillmann, H.; Abel, M.; Barth, J. V.; Kern, K. *J. Am. Chem. Soc.* **2002**, *124*, 14000.

(22) Lukas, S.; Witte, G.; Woll, C. *Phys. Rev. Lett.* **2002**, *88*, 028301.

(23) Nitschke, J. R.; Lehn, J. M. *Proc. Natl. Acad. Sci. U.S.A.* **2003**, *100*, 11970.

(24) Steiner, T. *Angew. Chem., Int. Ed.* **2002**, *41*, 48.

(25) Dietrichbuchecker, C. O.; Guilhem, J.; Pascard, C.; Sauvage, J. P. *Angew. Chem., Int. Ed.* **1990**, *29*, 1154.

(26) Davies, S. C.; Durrant, M. C.; Hughes, D. L.; Leidenberger, K.; Stapper, C.; Richards, R. L. *Dalton Trans.* **1997**, 2409. Chung, Y. H.; Wei, H. H.; Lee, G. H.; Wang, Y. *Inorg. Chim. Acta* **1999**, *293*, 30.

(27) Kern, K.; Zeppenfeld, P.; David, R.; Comsa, G. *Phys. Rev. Lett.* **1987**, *59*, 79.

(28) Hahn, E.; Kampshoff, E.; Fricke, A.; Bucher, J.-P.; Kern, K. *Surf. Sci.* **1994**, *319*, 277. Kern, K.; Niehus, H.; Schatz, A.; Zeppenfeld, P.; Goerge, J.; Comsa, G. *Phys. Rev. Lett.* **1991**, *67*, 855.

(29) Vanderbilt, D. Mesoscopic Ordering from Elastic and Electrostatic Interactions at Surfaces. In *Computations for the Nano-Scale*; Blochl, P. E., Ed.; Kluwer Academic Publishers: Netherlands, 1993; pp 1.